VERIFICATION OF THE NUCLEAR COMPUTATIONAL CODES LEOPARD, WIMS, AND MCNP THROUGH COMPARISON WITH EXPERIMENTAL CRITICALITY DATA

Amal S. Dakhil¹ and Entesar H. Ben Saad²

¹Department of Nuclear Engineering, Faculty of Engineering, University of Tripoli, Libya ²Radiation Medical Physics and Cyclotron Department, Tripoli university hospital Email: a.dakhil@uot.edu.ly

Received 23 April 2025; Revised 15 October 2025; Accepted 7 November 2025; Published 10 November 2025

الملخص

بُذلت خلال العقود الماضية جهودٌ كبيرة لتطوير والتحقق من دقة أكواد حساب نقل النيوترونات المستخدمة في تصميم المفاعلات النووية. كما أُجريت العديد من الحسابات النيترونية الدقيقة باستخدام طرائق محددة ومكتبات بيانات نووية خاصة، ومع ذلك، فإن الاستخدام المتكرر لأنظمة الأكواد الحالية في حساب تكوينات المفاعلات المختلفة يتطلب تحققًا وتأكيدًا مستمرين وصارمين لجودة النتائج، خاصةً عند استخدام بيانات نووية جديدة. تهدف هذه الدراسة إلى توضيح الفروقات بين القيم التي تم الحصول عليها من الأكواد الحاسوبية: "EOPARD, WIMS, MCNP code مقارنة بالنتائج التجريبية، إضافةً إلى تقييم دقة مكتبات المقاطع العرضية المستخدمة في كل كود. ولتحقيق بالنتائج التجريبية، إضافةً إلى تقييم دقة مكتبات المقاطع على غيره أو التقليل من أهمية الأكواد الأخرى، للمقارنة. لا تهدف الدراسة إلى تفضيل كود معين على غيره أو التقليل من أهمية الأكواد الأخرى، ولا إلى استبعاد أي كود من الاعتبار، بل تسعى إلى تقديم تقييم شامل لأدائها. أظهرت النتائج أداءً ممتازًا لجميع الأكواد، مما يقدم دليلاً مشجعًا للغاية على موثوقيتها. ويدعم استخدامها بدرجة عالية من الثقة كأدوات أساسية في دراسة تطبيقات النيترونات.

ABSTRACT

A lot of effort was devoted in the past to the development and to the validation of adequate neutron transport calculation codes for design calculation of nuclear reactors, and various accurate neutronic calculations have been performed using specific methods and nuclear data libraries. However, the frequent use of the existing code systems for calculations of reactors configurations requires a continuous and rigorous verification and validation of the quality of the results, especially when new nuclear data are used. This study aims to demonstrate the variations between the values obtained from computational codes LEOPARD, WIMS, and MCNP and the corresponding experimental results, as well as to evaluate the accuracy of the cross-section libraries utilized by each code. To achieve this, criticality experiments were chosen as the most appropriate benchmark for comparison. The study does not aim to declare a single code as the best or to undermine the significance of others, nor to exclude any code from consideration. Rather, it seeks to provide a comprehensive assessment of their performance. The results revealed very good performance across all codes, strong evidence of their reliability. This supports their use with a significant degree of confidence as essential tools for studying neutron applications.

KEYWORDS: TRX, multiplication factor, LEOPARD, WIMS, MCNP, computer code, criticality experiments.

INTRODUCTION

Engineering problems, especially in the nuclear field, ultimately rely on numerical solutions, as analytical methods are inherently limited. When a problem grows in complexity, with increasing variables and constants, finding an analytical solution becomes impossible, making numerical solutions the only feasible option. There are numerous Fortran programs designed to solve the multi-group diffusion and transport equation in one, two, or even three dimensions. Due to the large size of these programs, the variety of options they offer, and their ability to account for detailed aspects of different geometric shapes, they have come to be referred to as "codes" [1]. These codes model physical systems, specifically nuclear reactors in this context. They are used to simulate nuclear reactor systems at every stage, whether in design, operation, or refueling. Additionally, they calculate values of key physical factors necessary for sustaining the reaction within the reactor and verify the accuracy of results obtained from experimental trials. Through this study, the results of each code were compared with one another, allowing for an understanding of the nature and physics of each code, as well as the differences that exist between them. The impact of the nuclear libraries from which the codes derive the necessary data was also examined. The goal is to enhance confidence in these codes, which are primarily used in neutron analysis for nuclear reactors.

CODES USED

LEOPARD Code

LEOPARD is a unit-cell code that calculates neutron spectrum and multi-group diffusion constants for different materials in the light water reactors; it utilizes two-energy or four-energy group cross section sets. The code can also compute fuel depletion histories for a zero-dimensional system [2]. Figure (1) presents a general overview of LEOPARD's input and output structure while Figure (2) illustrates the flowchart of the LEOPARD libraries and its associated computational processes.

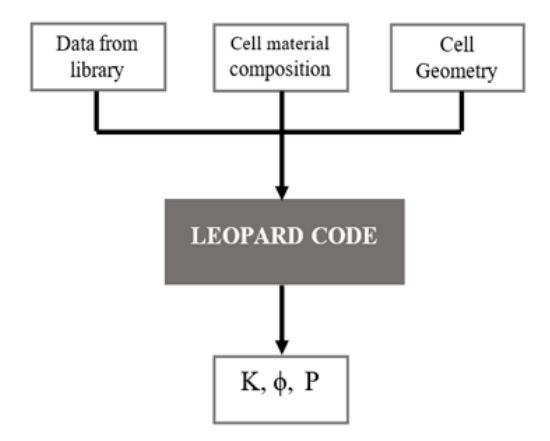


Figure 1: General chart of the input and output for LEOPARD code.

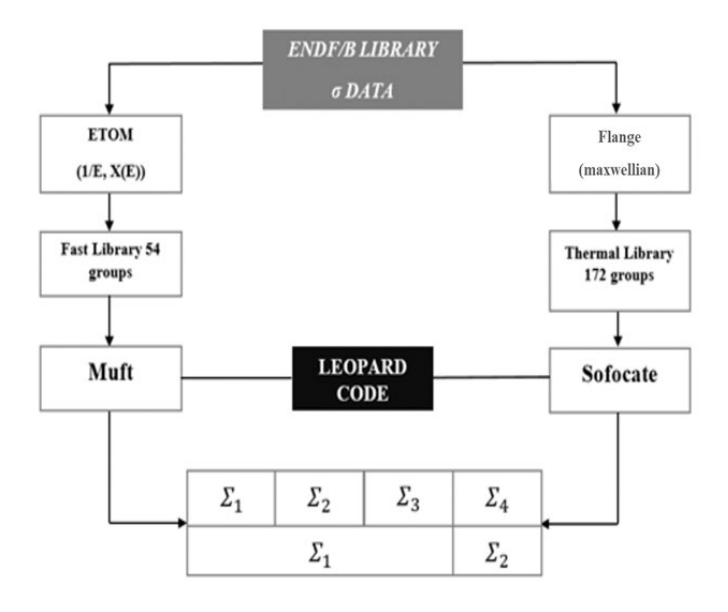


Figure 2: Flow chart for LEOPARD libraries.

WIMS Code

The Winfrith Improved Multi-Group Scheme (WIMS) code has been used extensively throughout the world for power and research reactor lattice physics analysis. WIMS applies transport theory to determine the neutron flux as a function of energy and spatial location in a one-dimensional cell. Two main transport options that are most frequently used are DSN (discrete ordinates) and PERSEUS (collision probabilities). The transport solution can be performed with any user specified group structure up to 69-groups or 172-groups [3]. Figure (3) presents a general overview of the input and output structure for the WIMS code.

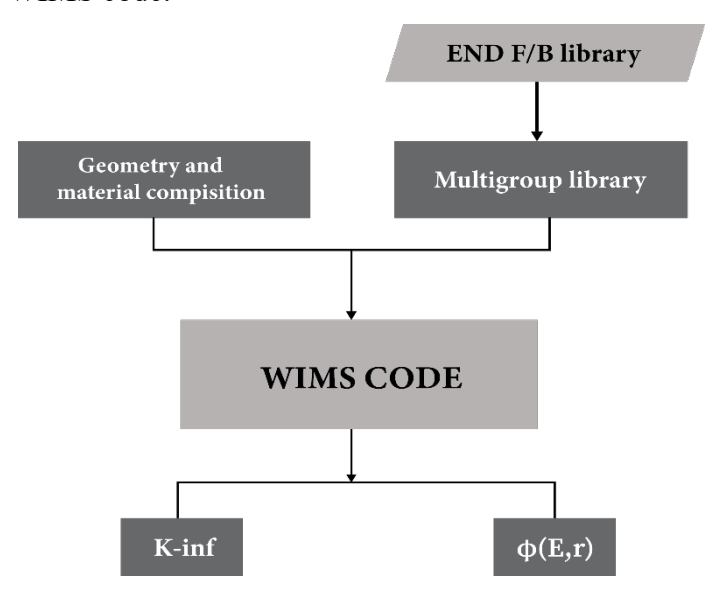


Figure 3: General chart of the input and output for WIMS code.

MCNP Code

MCNP (Monte Carlo N-particle) is a general-purpose, continuous-energy, generalized-geometry, time-dependent, coupled neutron/photon/electron Monte Carlo transport code. It can be used in several transport modes: neutron only, photon only, electron only, combined neutron/photon transport where the photons are produced by neutron interactions, neutron/photon/electron, photon/electron, or electron/photon. The neutron energy regime is from 10^{-11} MeV to 20 MeV, and the photon and electron energy regimes are from 1 keV to 1000 MeV. The capability to calculate $k_{\rm eff}$ eigenvalues for fissile systems is also a standard feature [4]. Figure (4) illustrates the general input structure and a portion of the output for the MCNP code.

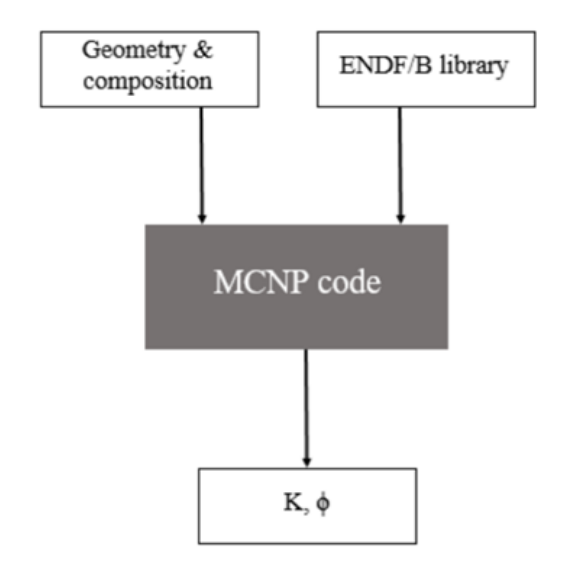


Figure 4: General chart of the input and a part of output for MCNP code.

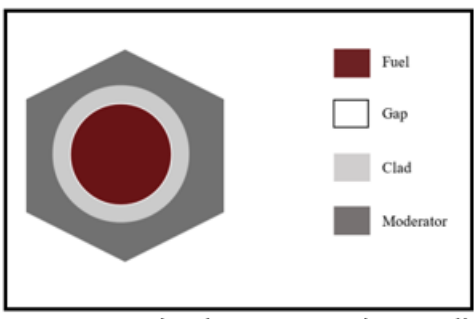
DATA USED

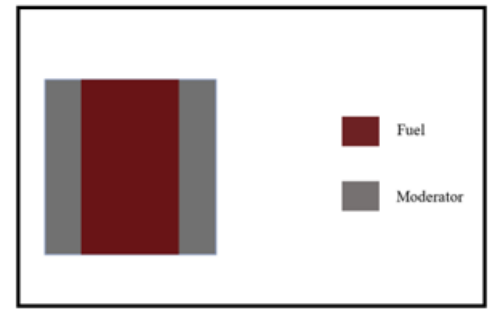
The TRX (Thermal Reactor One-Region Lattice) critical lattice experiments are a set of benchmark studies designed to validate reactor physics codes and nuclear data libraries. They focus on light water reactor physics using thermal neutron lattices. These experiments were performed in the 1960's at Bettis Atomic Power Laboratory [5]. Table (1) presents the specifications of the TRX unit cells [6], while Figure (5) shows the geometric shape of a TRX unit cell.

It should be noted that, in the TRX benchmark specifications, the natural uranium slab cell does not include a cladding layer. Figure 5a illustrates the TRX-Metal and TRX-UO2 rod-type cells, which are surrounded by an aluminum cladding, while Figure 5b represents a homogeneous fuel-moderator system where the fuel and moderator are in direct contact. Therefore, in all corresponding models and calculations, no cladding region was defined for the slab cell, in accordance with the experimental setup.

Table 1: TRX unit cells specifications [6].

| Parameter | Value | | | | |
|------------------------------------|---|--|--|--|--|
| | TRX metal | | | | |
| Atomic density of U ²³⁵ | $6.253 \times 10^{20} \text{atoms.cm}^{-3}$ | | | | |
| Atomic density of U ²³⁸ | $4.7205 \times 10^{22} \text{atoms.cm}^{-3}$ | | | | |
| Atomic density of Al ²⁷ | $6.025 \times 10^{22} \text{atoms.cm}^{-3}$ | | | | |
| Fuel radius | 0.4915 cm | | | | |
| Clad inner radius | 0.5042 cm | | | | |
| Clad outer radius | 0.5753 cm | | | | |
| Fuel rod length | 122.00 cm | | | | |
| Total buckling | 0.0057 cm ⁻² | | | | |
| TRX | | | | | |
| Atomic density of U ²³⁵ | $3.112 \times 10^{20} \text{atoms.cm}^{-3}$ | | | | |
| Atomic density of U ²³⁸ | $2.31270 \times 10^{22} \mathrm{atoms.cm^{-3}}$ | | | | |
| Atomic density of O ¹⁶ | $4.69460 \times 10^{22} \text{atoms.cm}^{-3}$ | | | | |
| Atomic density of Al ²⁷ | $6.025 \times 10^{22} \text{atoms.cm}^{-3}$ | | | | |
| Fuel radius | 0.4864 cm | | | | |
| Clad inner radius | 0.5042 cm | | | | |
| Clad outer radius | 0.5753 cm | | | | |
| Fuel rod length | 122.00 cm | | | | |
| Total buckling | 0.0057 cm ⁻² | | | | |
| Natural ura | | | | | |
| Atomic density of U ²³⁵ | $3.401 \times 10^{22} \text{atoms.cm}^{-3}$ | | | | |
| Atomic density of U ²³⁸ | $4.74830 \times 10^{22} \text{atoms.cm}^{-3}$ | | | | |
| Slab thickness | 2.54 cm | | | | |
| Slab length | 61cm × 61 cm | | | | |
| Total buckling | - 0.0013 cm ⁻² | | | | |
| Mode | erator | | | | |
| Atomic density of H ² | 0.06676 atoms.cm ⁻³ | | | | |
| Atomic density of O ¹⁶ | 0.03338 atoms.cm ⁻³ | | | | |





a- TRX-Metal and TRX-UO2 rod-type cell

b- Natural uranium slab cell

Figure 5: TRX unit cell shape.

CRITICALITY CALCULATIONS

The key parameter to be determined in this study is the multiplication factor. It will be evaluated using each of the implemented codes, as well as through a mathematical model that simulates their operation. The following section presents the equations used to calculate the multiplication factor based on both one-group and two-group cross-section data.

One-Group Criticality [1]

Based on the general definition of the effective multiplication factor:

$$K = \frac{\text{Production rates}}{\text{Loss rates}} = \frac{\text{Fission}}{\text{Leakage+Absorption}} = \frac{v \Sigma_f \phi(x)}{-D \frac{d^2 \phi}{dx^2} + \Sigma_a \phi(x)}$$
(1)

Thus, the effective multiplication factor and the infinite multiplication factor for the one-group criticality model are given by: $K = \frac{v\Sigma_f}{\Sigma_a} \cdot \frac{1}{1+L^2B_q^2}$ with $K_{\infty} = \frac{v\Sigma_f}{\Sigma_a}$

Two-Group Criticality [1]

To analyze a bare core for a two-group criticality analysis, we can make the following assumptions to simplify the development of the criticality equation: a uniform medium, a non-critical reactor, no up scattering, and no fission neutrons born in a thermal group.

The equations take the following form:

$$-D_1 \nabla^2 \phi_1(\underline{r}) + \Sigma_{R1} \phi_1(\underline{r}) = \frac{1}{\nu} \left[\nu_1 \Sigma_{f1} \phi_1(\underline{r}) + \nu_2 \Sigma_{f2} \phi_2(\underline{r}) \right] \tag{2}$$

$$-D_2 \nabla^2 \phi_2(r) + \Sigma_{a2}(r) \phi_2(r) = \Sigma_{s12} \phi_1(r)$$
(3)

So, the effective multiplication factor and the infinite multiplication factor based on two group is:

$$K = \frac{v_2 \Sigma_{f2}}{\Sigma_{a2}} \cdot \frac{\Sigma_{S12}}{\Sigma_{a1} + \Sigma_{S12}} \cdot \frac{1}{[1 + L_1^2 B_q^2]} \cdot \frac{1}{[1 + L_2^2 B_q^2]} \text{ and } K_{\infty} = \frac{v_2 \Sigma_{f2}}{\Sigma_{a2}} \cdot \frac{\Sigma_{S12}}{\Sigma_{a2} + \Sigma_{S12}}$$

RESULTS AND DISCUSSION

In this section, the results obtained from this study are discussed by conducting a comparison between the values from all three codes, whether obtained directly or through mathematical models.

Comparison of Results Derived from Mathematical Models

The primary objective of these calculations is to gain a deeper understanding of the nature of deterministic codes, which in turn allows for a fairer and more accurate evaluation of their performance. To calculate the multiplication factor for the deterministic codes, it is essential to first determine the cross-section values. Therefore, the cross-sections for both the two-group and one-group models were obtained from the WIMS and LEOPARD codes. Tables (2&3) present the cross-section values for LEOPARD code in the two-group and one-group models, respectively.

Table 2: Two-group cross sections obtained using the LEOPARD code.

| | Pitch (cm) | \sum_{a1} (cm ⁻¹) | $\sum_{S12} (\text{cm}^{-1})$ | $\nu \sum_{f1} (\text{cm}^{-1})$ | \sum_{a2} (cm ⁻¹) | $\nu \sum_{f2} (\text{cm}^{-1})$ |
|------------------------|------------|---------------------------------|-------------------------------|----------------------------------|---------------------------------|----------------------------------|
| TRX | 1.806 | 0.011 | 0.026 | 0.008 | 0.101 | 0.142 |
| metal | 2.174 | 0.008 | 0.033 | 0.006 | 0.076 | 0.098 |
| TRX UO ₂ | 1.806 | 0.007 | 0.028 | 0.004 | 0.062 | 0.081 |
| Natural | 2.7868 | 0.013 | 0.023 | 0.010 | 0.076 | 0.082 |
| slab | 1.270 | 0.017 | 0.012 | 0.011 | 0.113 | 0.137 |

Table 3: One-group cross section using the LEOPARD code.

| | Pitch (cm) | D (cm) | $\sum_a (\text{cm}^{-1})$ | $\nu \sum_f (\text{cm}^{-1})$ |
|---------------------|------------|--------|---------------------------|-------------------------------|
| TDX 1 | 1.806 | 1.016 | 0.029 | 0.035 |
| TRX metal | 2.174 | 0.923 | 0.028 | 0.033 |
| TRX UO ₂ | 1.8060 | 1.142 | 0.024 | 0.027 |
| Natural | 2.7686 | 0.667 | 0.022 | 0.022 |
| slab | 1.270 | 0.880 | 0.026 | 0.024 |

Tables (4&5) present the cross-section values for WIMS code in the two-group and one-group models, respectively.

Table 4: Two-group cross sections obtained using the WIMS code.

| | Pitch (cm) | \sum_{a1} (cm ⁻¹) | $\sum_{S12} (\text{cm}^{-1})$ | $ u \sum_{f1} (\text{cm}^{-1}) $ | \sum_{a2} (cm ⁻¹) | $\nu \sum_{f2} (\text{cm}^{-1})$ |
|---------------------|------------|---------------------------------|-------------------------------|----------------------------------|---------------------------------|----------------------------------|
| TRX metal | 1.806 | 0.007 | 0.0887 | 0.016 | 0.037 | 0.041 |
| 1 KA metai | 2.174 | 0.0057 | 0.0937 | 0.012 | 0.035 | 0.039 |
| TRX UO ₂ | 1.806 | 0.004 | 0.0807 | 0.008 | 0.029 | 0.032 |
| Natural | 2.7686 | 0.007 | 0.0978 | 0.016 | 0.031 | 0.026 |
| slab | 1.270 | 0.0107 | 0.091 | 0.026 | 0.035 | 0.030 |

Table 5: One-group cross section using the WIMS code.

| | Pitch (cm) | D (cm) | $\sum_a (\text{cm}^{-1})$ | $\nu \sum_f (\text{cm}^{-1})$ |
|---------------------|------------|--------|---------------------------|-------------------------------|
| TRX | 1.806 | 1.121 | 0.031 | 0.035 |
| metal | 2.174 | 1.008 | 0.027 | 0.032 |
| TRX UO ₂ | 1.806 | 1.043 | 0.022 | 0.026 |
| Natural | 2.7686 | 0.860 | 0.025 | 0.024 |
| slab | 1.270 | 0.985 | 0.028 | 0.029 |

Since all TRX benchmark configurations represent critical systems, the experimentally measured effective multiplication factor is $k_{\rm eff} = 1.000$. Therefore, all calculated $k_{\rm eff}$ values in this study are compared against this reference value. The percentage deviations shown in parentheses are calculated using:

% Deviation =
$$|k_{calc} - 1| \times 100$$

Tables (6&7) summarize the calculated $k_{\rm eff}$ values for the different benchmark configurations using the LEOPARD and WIMS codes.

Table 6: Comparison of the calculated $k_{\rm eff}$ based on one-group cross section results.

| | Pitch (cm) | LEOPARD code | WIMS code |
|---------------------|------------|--------------|--------------|
| TRX metal | 1.806 | 0.999 (0.1%) | 0.937 (6.3%) |
| TRA metai | 2.174 | 0.991 (0.9%) | 0.979 (2.1%) |
| TRX UO ₂ | 1.806 | 0.910 (9.0%) | 0.901 (9.9%) |
| Natural slab | 2.7686 | 1.010 (1%) | 1.003 (0.3%) |
| | 1.27 | 0.949 (5.1%) | 1.069 (6.9%) |

Table (7) shows a comparison of the calculated $k_{\rm eff}$ values based on two-group cross sections from both LEOPARD and WIMS codes.

Table (8) presents a comparison of the $k_{\rm eff}$ results obtained using the three different codes (LEOPARD, WIMS and MCNP).

Table 7: Comparison of the calculated $k_{\rm eff}$ based on two-group cross sections.

| | Pitch (cm) | LEOPARD code | WIMS code |
|---------------------|------------|--------------|--------------|
| | 1.806 | 0.995 (0.5%) | 0.952(4.8%) |
| TRX metal | 2.174 | 0.987 (1.3%) | 0.945 (5.5%) |
| TRX UO ₂ | 1.806 | 0.906 (9.4%) | 0.906 (9.4%) |
| Natural slab | 2.7686 | 1.010 (1%) | 0.966 (3.4%) |
| | 1.27 | 1.041 (4.1%) | 1.061 (6.1%) |

Table 8: Comparison of $k_{\rm eff}$ values from various codes using two-group cross sections.

| | Pitch | LEOPARD code | WIMS code | MCNP code |
|---------------------|--------|---------------|--------------|--------------|
| | 1.806 | 0.999 (0.1%) | 0.995 (0.5%) | 1.002 (0.2%) |
| TRX metal | 2.174 | 0.991 (0.9%) | 0.995 (0.5%) | 0.993 (0.7%) |
| TRX UO ₂ | 1.806 | 0.908 (9. 2%) | 0.921 (7.9%) | 0.972 (2.8%) |
| | 2.7686 | 1.009 (0.9%) | 0.966 (3.4%) | 0.999 (0.1%) |
| Natural slab | 1.27 | 0.947 (5.3%) | 1.061 (6.1%) | 1.012 (1.2%) |

As shown in Table 8, the MCNP results exhibit the closest agreement with the experimental criticality values for all TRX configurations. The deviations obtained with MCNP remain relatively small, not exceeding 3%, and are consistently lower than those produced by the deterministic codes (LEOPARD and WIMS), which exhibited larger deviations, particularly for the TRX-UO₂ case, where the difference reached about 7–9%. Therefore, the preference for the MCNP code in this study is based on its superior consistency with the experimental data, thereby demonstrating higher accuracy under identical benchmark conditions.

Based on the results presented in Table (8), it can be concluded that all the codes performed very well, showing excellent agreement with the experimental data. Therefore, all the codes can be considered successful. However, if one code were chosen based on the accuracy of the results, the MCNP code would undoubtedly be selected for the following reasons:

1. The solution methods:

The WIMS and LEOPARD codes are deterministic methods. As a result, various mathematical simplifications are applied to the neutron transport equation to facilitate its

solution. These simplifications contribute to an increased margin of error, making the results less representative of the real case. On the other hand, the MCNP code uses a stochastic method (random walk), simulating the actual physical system by relying on statistical methods. As a result, the error rate in this case is remarkably low compared to the error rate associated with deterministic methods.

2. Cross section libraries:

As mentioned previously, nuclear data (cross-sections) are collected and stored in the ENDF/B library in a continuous-energy format. However, deterministic codes cannot directly process this data. Therefore, a procedure known as the averaging technique is applied to divide the energy range into discrete groups. This process combines multiple microscopic cross-section values into a single averaged value for each group, introducing an additional source of uncertainty. This approach is employed in both the WIMS and LEOPARD codes. The LEOPARD code uses a thermal library with 172 energy groups, and a fast library with 54 energy groups. The WIMS code, on the other hand, uses a 172-group structure, composed of 80 thermal groups, 47 resonance groups, and 45 fast groups. In the case of the MCNP code, the situation is different.

Monte Carlo method codes do not face difficulties in handling the ENDF/B library. Therefore, the MCNP code directly retrieves the nuclear data it requires from the library. As a result, MCNP avoids the uncertainties associated with energy-group averaging and provides higher accuracy in neutron transport calculations. As an illustration, Table (9) presents the total number of tabulated data points for the cross-section of selected isotopes in the MCNP nuclear data library [4].

| Table 9: Tabulated d | ata points for selected | l isotopes in the MCN | IP library [4]. |
|----------------------|-------------------------|-----------------------|-----------------|
| | Element | Total length | |

| Element | Total length |
|--------------------|--------------|
| U^{235} | 289,975 |
| U^{238} | 206,322 |
| AL^{27} | 55,427 |
| O^{16} | 58,253 |
| H^2 | 3,484 |

The total length represents the number of tabulated cross-section data points in the nuclear data file for each isotope (dimensionless).

3. The ability to represent real-world systems:

The ability of the codes to represent real-world systems affects the accuracy of the results. LEOPARD is a zero-dimensional code, which fundamentally restricts its ability to model realistic systems. While WIMS, as a one-dimensional code, offers some improvement, it remains inadequate in fully representing the complexities of real-world systems. In contrast, MCNP code, being a three-dimensional code, provides a much more accurate representation of real-world systems, effectively reducing errors associated with dimensional approximations.

Although the MCNP code was chosen, this does not mean that the other codes are unimportant or that their results are unreliable. In fact, despite the mathematical simplifications and the specialized handling of nuclear data, the results continue to be highly accurate and valuable.

CONCLUSION

The use of numerical solutions in neutron applications is considered essential due to the complexity and detailed nature of nuclear reactor systems. The mathematical modeling of such intricate environments is challenging, making the adoption of computational software a necessity rather than a luxury. Consequently, it is crucial to assess the ability of these software tools to simulate reactor systems accurately.

The primary objective of this work is to evaluate the extent of variation in the results produced by these codes compared to experimental data. The aim of this study is not to declare any specific code as superior or definitive.

Despite differences in their methodologies, all the codes evaluated in this study have shown excellent results, providing confidence in their use for neutron applications. However, if a single code must be selected as the primary choice, MCNP code would be the preferred option due to the following reasons: its solution methodology, the accuracy of its cross-section library, and its capability to simulate real-world systems effectively.

NOMENCLATURE

K = effective multiplication factor.

 $K\infty$ = infinite multiplication factor.

 Σ_f = macroscopic fission cross section (cm⁻¹).

 Σ_a = macroscopic absorption cross section (cm⁻¹).

D = neutron diffusion coefficient (cm).

 $\phi(x)$ = neutron flux at position x (n/cm²·s).

L = diffusion length (cm), where $L^2 = D / \Sigma_a$.

 B_q^2 = geometrical buckling (cm⁻²).

 D_1 , D_2 = diffusion coefficients for fast and thermal groups (cm).

 ϕ_1 , ϕ_2 = neutron fluxes in fast and thermal groups (n/cm²·s).

 Σ_{a1} , Σ_{a2} = macroscopic absorption cross section for fast and thermal group (cm⁻¹).

 Σ_{f1} , Σ_{f2} = macroscopic fission cross sections for fast and thermal groups (cm⁻¹).

 v_1, v_2 =average number of neutrons emitted per fission in fast and thermal groups.

 Σ_{s12} = transfer scattering cross section from fast to thermal groups (cm⁻¹).

 Σ_{R1} = removal cross section for fast group (cm⁻¹).

 L_1 , L_2 = diffusion lengths for fast and thermal groups (cm).

REFERENCES

- [1] Kuridan, R. (2004). *Nuclear Reactor Theory* (in Arabic). National Office for Research and Development, Tripoli.
- [2] Barry, R. F. (1964). *LEOPARD: A Spectrum Dependent Non-Spatial Depletion Code*. Bettis Atomic Power Laboratory, West Mifflin.
- [3] Deen, J. R., and Woodruff, W. L. (1995). *WIMS-D4M User Manual, Revision 0.* Argonne National Laboratory, Argonne, Illinois.
- [4] Pelowitz, D. B. (2005). *MCNPX User's Manual, Version 2.6*. Los Alamos National Laboratory, Los Alamos.
- [5] Khan, M. J. H., Alam, A. B., Ahsan, M. H., Mamun, K. A. and Islam, S. M. (2015). Validation Study of the Reactor Physics Lattice Transport Code WIMSD-5B by TRX and BAPL Critical Experiments of Light Water Reactors. *Journal of Nuclear Science and Technology*, 52 (4), 455–462.
- [6] Hardy, J., Klein, D., and Volpe, J. Jr. (1970). A Study of Physics Parameters in Several Water-Moderated Lattices of Slightly Enriched and Natural Uranium. Oak Ridge: Oak Ridge National Laboratory.